



ACADEMIC
PRESS

Available online at www.sciencedirect.com

SCIENCE @ DIRECT®

Journal of Sound and Vibration 269 (2004) 727–743

JOURNAL OF
SOUND AND
VIBRATION

www.elsevier.com/locate/jsvi

Determination of optimal exciter deployment for panel speakers using the genetic algorithm

Mingsian R. Bai*, Bowen Liu

*Department of Mechanical Engineering, National Chiao-Tung University, 1001 Ta-Hsueh Road,
Hsin-Chu 300, Taiwan, ROC*

Received 29 August 2002; accepted 23 January 2003

Abstract

A large multi-exciter panel speaker has been constructed in this work. In order to achieve the best design, an optimization procedure using the genetic algorithm (GA) has been developed. A total numerical model was first established for simulation, where the electrical system, the mechanical system, and the acoustical coupling in the panel speaker are accounted for within a coupled framework. Performance indices including the frequency response, the sound power, and the directional response are calculated. The simulation model also serves as the basis for the optimal design that aims at achieving omni-directional responses at high efficiencies. A GA-based optimization scheme was exploited to search for the positions of exciters and the delays of input signals which render the optimal performance. The optimal design was verified by experimental investigations. The results indicate that the optimal configuration indeed produced better performance in terms of efficiency and omni-directionality than the non-optimal one.

© 2003 Elsevier Science Ltd. All rights reserved.

1. Introduction

Panel speakers have attracted some research interest in recent years. The basic structure of a panel speaker generally consists of a panel and one or several inertia exciters (Fig. 1). The advantages of panel loudspeakers compared with conventional loudspeakers are compactness, omni-directionality, linear on-axis, attenuation, insensitivity to room conditions, bi-polar radiation, good linearity, and so forth [1]. Potential applications of panel speaker encompass multimedia, high-fidelity audio systems, public addressing systems, projection screens, LCD monitor speakers, and so forth.

*Corresponding author. Fax: +886-3-5720634.

E-mail address: msbai@mail.nctu.edu.tw (M.R. Bai).

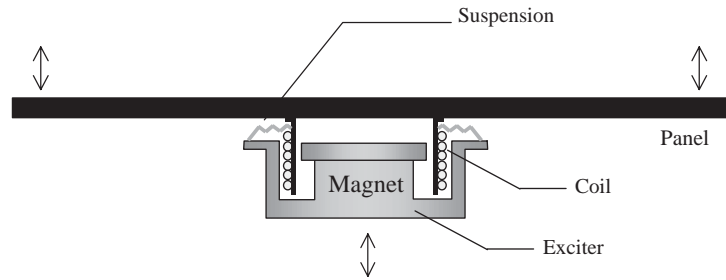


Fig. 1. Structure of the panel speaker. A panel speaker consists of a panel, one or more exciters.

Despite all the merits claimed by the supporters of panel speakers, there is still one unresolved problem that needs to be addressed before we find ubiquitous use of the newly advent device. Although panel loudspeakers have less beaming problem in high frequency, they generally suffer from another problem of efficiency due to hydrodynamic short circuit below coincidence frequency [2]. The physical constraint pertaining to the panel speaker hinders itself from being an ideally omni-directional and full-range device. This motivates the development of a systematic yet practical optimization scheme in this paper that seeks to best trade-off the omni-directionality and the efficiency by choosing appropriate exciter positions and electronic compensation.

A numerical model was first developed as the basis of the optimization procedure. In contrast to the simplified approach used in Ref. [2] which neglected the effect of acoustic coupling, this paper treats the electrical, mechanical, and acoustical systems as a coupled system. Various approaches dealing with sound–structure interactions can be found in literature [3–5]. In this work, impedance matrices of the exciters, the panel, and the medium are combined into a total impedance matrix for the coupled analysis. To simplify the calculation, the assumed-modes method is used in generating a structure model of the panel. Electro-mechanical analogy is also utilized to model the exciters. A discrete version of the Rayleigh’s integral is used to account for the effect of acoustic loading. The frequency response, the sound power and the directional response of the panel speaker can be calculated using this numerical model.

On the basis of the numerical model, an optimization procedure was then developed to reach the best compromise between the omni-directionality and efficiency. Instead of the “golden aspect ratio” used in the conventional isotropic panel speaker design, the optimization procedure was exploited to find the best positions to deploy exciters and the best electronic compensation (pure delays in our work) to the input signal, such that the beaming problem at high frequencies is alleviated, with maximal output of acoustic power. In this paper, the genetic algorithm (GA), an optimization technique based on the law of the evolution of species by natural selection, is adopted in the optimization procedure [6]. The thus obtained optimal design was verified experimentally in this paper. The results show that the optimal design indeed produced better performance in terms of the efficiency and the omni-directionality than the non-optimal design. The results will be discussed and summarized in the conclusion.

2. Modelling of panel speakers

In this section, details of the dynamic model of the panel–exciter system are given, with the acoustic coupling taken into account. The impedance approach is presented for the analysis of the coupled system.

2.1. Coupled system analysis of a multiply excited panel speaker

Consider a fluid-loaded thin panel depicted in Fig. 2. The panel is divided into N elements with the same area. Assume that the panel is subjected to external concentrated forces due to exciters. Let $\mathbf{f} = [f_1 \ f_2 \ \dots \ f_N]^T$ and $\mathbf{v} = [u_1 \ u_2 \ \dots \ u_N]^T$ be the force vector and the velocity vector associated with the center of each element on the panel surface. By certain discretization scheme, there exists the following relation between \mathbf{f} and \mathbf{v} [3–5]:

$$\mathbf{Z}_m \mathbf{v} = \mathbf{f} - \mathbf{Z}_a \mathbf{v}, \tag{1}$$

where \mathbf{Z}_m is the mechanical impedance matrix of the panel and \mathbf{Z}_a is the radiation impedance matrix. Note that all forces are expressed in the concentrated form. Hence,

$$(\mathbf{Z}_m + \mathbf{Z}_a) \mathbf{v} = \mathbf{f}. \tag{2}$$

Next, electro-mechanical analogy is employed for modelling the exciters. The exciters are assumed to be floating and the magnets of the exciters serve as a proof masses to produce inertia force. The exciter can be modelled by the equivalent circuit (mobility analogy) in Fig. 3(a). In this figure, $Z_c = R_c + j\omega L_E$ is the electrical impedance of the voice coil. Bl is the motor constant of the voice coil. C_s and R_s are the compliance and the damping, respectively, between the magnet and the panel. M_m is the mass of the magnet assembly. M_c is the mass of the voice coil. In Fig. 3(b), the equivalent circuit is reflected to the mechanical side, where f_b is the equivalent blocked force reflected to the mechanical side, Z_x is the equivalent impedance of the exciter, and Z_{Load} is the loading experienced by the exciter, including the mechanical loading and the acoustic loading. The relation between f_b and f is

$$f = f_b - Z_x u. \tag{3}$$

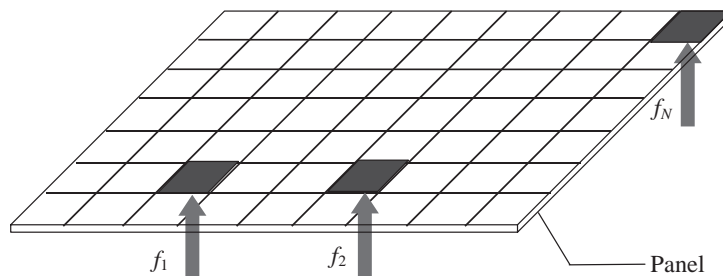


Fig. 2. A panel subjected to concentrated forces. The panel is discretized into N elements.

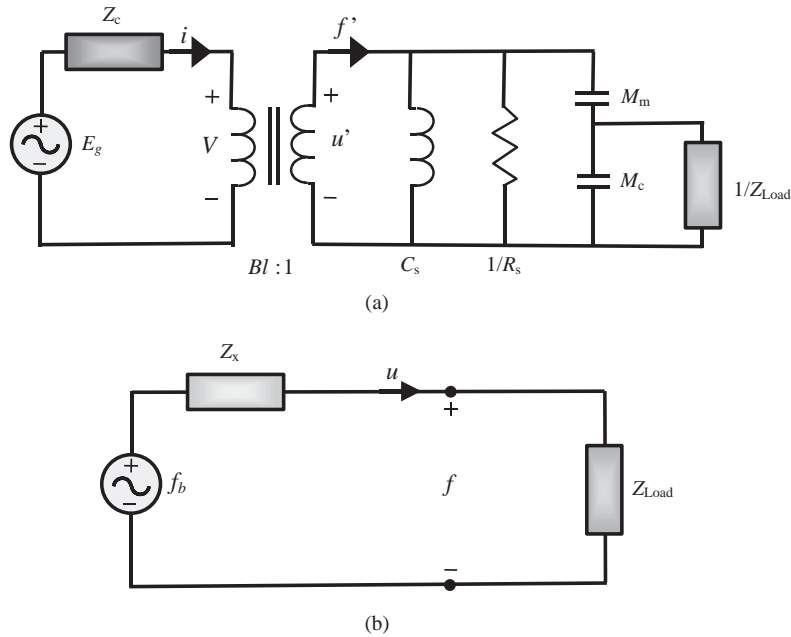


Fig. 3. Electro-mechanical analogy of a panel speaker: (a) equivalent circuit (mobility analogy) and (b) equivalent circuit reflected to mechanical side (impedance analogy). The symbols f and u in the figures denote, respectively, the force and the velocity.

With some algebraic manipulations, the impedance Z_x can be expressed as

$$Z_x = j\omega M_c + j\omega M_m \times \frac{(j\omega)^2 R_s C_s L_E + (j\omega)(R_c R_s C_s + B^2 l^2 C_s + L_E) + R_c}{(j\omega)^3 M_m C_s L_E + (j\omega)^2 (M_m C_s R_c + C_s L_E R_s) + (j\omega)(B^2 l^2 C_s + R_c R_s C_s + L_E) + R_c}. \quad (4)$$

The blocking force f_b can also be related to the input voltage source E_g as

$$f_b = \frac{(j\omega) E_g B l M_m C_s Z_x}{(j\omega)^2 M_m M_c C_s Z_c + (j\omega)(B^2 l^2 + R_s Z_c)(M_m + M_c) C_s + (M_m + M_c) Z_c}, \quad (5)$$

where $Z_c = R_c + j\omega L_E$, as defined previously, and Z_x is given in Eq. (4). Note that the above expression has a blocking zero at DC, which means that the inertia shaker is not able to supply a force to the panel at DC. This equation is only valid for one exciter. If we consider N exciters mounted on the panel, Eq. (3) should be modified into a matrix form

$$\mathbf{f} = \mathbf{f}_b - \mathbf{Z}_x \mathbf{v}, \quad (6)$$

where $\mathbf{f}_b = [f_{b1} \ f_{b2} \ \dots \ f_{bN}]^T$,

$$\mathbf{Z}_x = \begin{bmatrix} Z_{x1} & 0 & \dots & 0 \\ 0 & Z_{x2} & \ddots & \vdots \\ \vdots & \ddots & \ddots & 0 \\ 0 & \dots & 0 & Z_{xN} \end{bmatrix}. \quad (7)$$

Substituting Eq. (6) into Eq. (2) gives

$$(\mathbf{Z}_m + \mathbf{Z}_a)\mathbf{v} = \mathbf{f}_b - \mathbf{Z}_x\mathbf{v}. \tag{8}$$

Let $\mathbf{Z} = (\mathbf{Z}_m + \mathbf{Z}_a + \mathbf{Z}_x)$ be the total impedance matrix. We can finally arrive at the succinct relation

$$\mathbf{Z}\mathbf{v} = \mathbf{f}_b \tag{9}$$

from which one may derive the surface velocity of the panel from the known input voltage.

2.2. Mechanical impedance matrix of the panel (\mathbf{Z}_m)

Without fluid loading, the relation between the concentrated force vector \mathbf{f} and the velocity vector \mathbf{v} can be written as

$$\mathbf{f} = \mathbf{Z}_m\mathbf{v}. \tag{10}$$

In this paper, the assumed-modes method is employed to evaluate the mechanical impedance matrix \mathbf{Z}_m [7]. Consider a rectangular plate of the dimension $L_x \times L_y$. Using the assumed-modes method, we express the displacement of the plate as [7]

$$w(x, y, t) = \sum_{i=1}^{\ell} \phi_i(x, y)q_i(t), \tag{11}$$

where ℓ is the number of modes, $\phi_i(x, y)$ is the i th admissible function of the panel, and $q_i(t)$ is the generalized co-ordinate. The admissible functions can be found by analytical methods or numerical methods such as the finite-element method [8].

The strain energy of the plate is

$$U = \frac{D}{2} \int_0^{L_y} \int_0^{L_x} [w_{xx}^2(x, y, t) + w_{yy}^2(x, y, t) + 2\nu w_{xx}(x, y, t)w_{yy}(x, y, t) + 2(1 - \nu)w_{xy}^2(x, y, t)] dx dy, \tag{12}$$

where

$$D = \frac{Eh^3}{12(1 - \nu^2)} \tag{13}$$

is the bending stiffness of the plate. E , ν , and h are Young’s modulus, the Poisson ratio, and the thickness of the panel. The subscripts of w indicate differentiation of w with respect to that subscript. The kinetic energy is given by

$$T = \frac{1}{2} \int_0^{L_y} \int_0^{L_x} \mu w_t^2(x, y, t) dx dy, \tag{14}$$

where μ is the surface mass density. The virtual work done by the exciting force $f(x, y, t)$ is

$$\delta W = \int_0^{L_y} \int_0^{L_x} f(x, y, t)\delta w(x, y, t) dx dy. \tag{15}$$

Using the assumed-modes method, we can rewrite Eqs. (12), (14) and (15) as

$$U = \frac{1}{2} \sum_{i=1}^{\ell} \sum_{j=1}^{\ell} k_{ij} q_i(t) q_j(t), \quad (16)$$

where k_{ij} is the modal mass,

$$k_{ij} = D \int_0^{L_y} \int_0^{L_x} [\phi_{i,xx}(x, y) \phi_{j,xx}(x, y) + \phi_{i,yy}(x, y) \phi_{j,yy}(x, y) + 2\nu \phi_{i,xx}(x, y) \phi_{j,yy}(x, y) + 2(1 - \nu) \phi_{i,xy}(x, y) \phi_{j,xy}(x, y)] dx dy, \quad (17)$$

$$T = \frac{1}{2} \sum_{i=1}^{\ell} \sum_{j=1}^{\ell} m_{ij} \dot{q}_i(t) \dot{q}_j(t), \quad (18)$$

where m_{ij} is the modal stiffness,

$$m_{ij} = \mu \int_0^{L_y} \int_0^{L_x} \phi_i(x, y) \phi_j(x, y) dx dy, \quad (19)$$

$$\delta V = \sum_{i=1}^{\ell} f_i \delta q_i(t),$$

where

$$f_i = \int_0^{L_y} \int_0^{L_x} f(x, y, t) \phi_i(x, y) dx dy.$$

Define the Lagrangian $L = T - U$. The Lagrange's equation reads [9]

$$\frac{\partial}{\partial t} \left(\frac{\partial L}{\partial \dot{q}_i} \right) - \frac{\partial L}{\partial q_i} = f_i, \quad i = 1, \dots, \ell. \quad (20)$$

Substituting Eqs. (16), (18) and (19) into Eq. (20) leads to the following matrix differential equation:

$$\tilde{\mathbf{M}} \ddot{\mathbf{q}} + \tilde{\mathbf{K}} \mathbf{q} = \mathbf{f}, \quad (21)$$

where $\tilde{\mathbf{M}}$ is the modal mass matrix and $\tilde{\mathbf{K}}$ is the modal stiffness matrix. From Eq. (21), we can identify the modal mechanical impedance matrix of panel

$$\tilde{\mathbf{Z}}_m = \frac{\tilde{\mathbf{K}} - \omega^2 \tilde{\mathbf{M}}}{j\omega}. \quad (22)$$

On the other hand, Eq. (11) can be expressed in matrix notations

$$\mathbf{w} = \boldsymbol{\Phi} \mathbf{q}, \quad (23)$$

where

$$\boldsymbol{\Phi} = \begin{bmatrix} \phi_1(x_1, y_1) & \phi_2(x_1, y_1) & \cdots & \phi_\ell(x_1, y_1) \\ \phi_1(x_2, y_2) & \phi_2(x_2, y_2) & \cdots & \phi_\ell(x_2, y_2) \\ \vdots & \vdots & \ddots & \vdots \\ \phi_1(x_\ell, y_\ell) & \phi_2(x_\ell, y_\ell) & \cdots & \phi_\ell(x_\ell, y_\ell) \end{bmatrix} \quad (24)$$

is the modal matrix which is for convenience made to be square (number of elements = number of modes) and normalized into an orthogonal matrix, i.e., $\boldsymbol{\Phi}^T \boldsymbol{\Phi} = \boldsymbol{\Phi} \boldsymbol{\Phi}^T = \mathbf{I}$. Therefore, the mechanical impedance in the physical space and that in the modal space can be related by

$$\mathbf{Z}_m = \boldsymbol{\Phi} \tilde{\mathbf{Z}}_m \boldsymbol{\Phi}^T. \quad (25)$$

2.3. Radiation impedance matrix (\mathbf{Z}_a)

Let \mathbf{f}_a be equivalent concentrated forces due to acoustic pressure, acting on each element. There exists the following relation:

$$\mathbf{f}_a = \mathbf{Z}_a \mathbf{v}. \quad (26)$$

Many methods are available for calculating \mathbf{Z}_a . A simple technique described in Ref. [10] is used in our work to obtain the matrix \mathbf{Z}_a :

$$\mathbf{Z}_a = S \rho_0 c \begin{bmatrix} 1 - e^{-jk\sqrt{S/\pi}} & \frac{jkS e^{-jkr_{12}}}{2\pi r_{12}} & \cdots & \frac{jkS e^{-jkr_{1N}}}{2\pi r_{1N}} \\ \frac{jkS e^{-jkr_{21}}}{2\pi r_{21}} & 1 - e^{-jk\sqrt{S/\pi}} & \cdots & \vdots \\ \vdots & \vdots & \cdots & \vdots \\ \frac{jkS e^{-jkr_{N1}}}{2\pi r_{N1}} & \cdots & \cdots & 1 - e^{-jk\sqrt{S/\pi}} \end{bmatrix}. \quad (27)$$

S is the area of each element, r_{mn} is the distance from the center of the element n to the point m ($m, n = 1, \dots, N$).

2.4. Evaluation of the sound pressure and the sound power

The farfield pressure can be calculated using the propagation matrix \mathbf{E} :

$$\mathbf{p} = \mathbf{E} \mathbf{v}, \quad (28)$$

where \mathbf{p} is the farfield pressure vector and \mathbf{v} is the surface velocity vector of the panel [10]. For baffled radiators,

$$\mathbf{E} = j \frac{\rho_0 c k S}{2\pi} \begin{bmatrix} \frac{e^{-jkr_{11}}}{r_{11}} & \frac{e^{-jkr_{12}}}{r_{12}} & \dots & \frac{e^{-jkr_{1N}}}{r_{1N}} \\ \frac{e^{-jkr_{21}}}{r_{21}} & \frac{e^{-jkr_{22}}}{r_{22}} & \dots & \frac{e^{-jkr_{2N}}}{r_{2N}} \\ \vdots & \vdots & \dots & \vdots \\ \frac{e^{-jkr_{M1}}}{r_{M1}} & \frac{e^{-jkr_{M2}}}{r_{M2}} & \dots & \frac{e^{-jkr_{MN}}}{r_{MN}} \end{bmatrix}, \tag{29}$$

where r_{mn} is the distance from the center of the element n to the field point m ($m, n = 1, \dots, M$).

The radiated sound power can be calculated as

$$W = \mathbf{v}^H \mathbf{R} \mathbf{v}, \tag{30}$$

where $\mathbf{R} = \text{Re}\{\mathbf{Z}_a\}/2$, and the radiation resistance matrix \mathbf{R} is a positive definite matrix [10]:

$$\mathbf{R} = \frac{\omega^2 \rho S^2}{4\pi c} \begin{bmatrix} 1 & \frac{\sin(kr_{12})}{kr_{12}} & \dots & \frac{\sin(kr_{1N})}{kr_{1N}} \\ \frac{\sin(kr_{21})}{kr_{21}} & 1 & \dots & \vdots \\ \vdots & \vdots & \ddots & \vdots \\ \frac{\sin(kr_{N1})}{kr_{N1}} & \dots & \dots & 1 \end{bmatrix}. \tag{31}$$

2.5. Numerical simulation of the system response

In this section, simulations are conducted to verify the forgoing model of the panel speaker. Assume that the panel is of the dimension 0.27 m × 0.27 m. The core material of panel is PU foam. The parameters of the exciter and the panel measured from a real 25 mm voice coil are listed in Table 1. Although in principle admissible functions of any kind can be used in the assumed-modes method, the eigenfunctions of the simply supported plate are adopted in this paper because they are practical for efficient computation involved in the ensuing optimization. For a simply supported plate of dimension $L_x \times L_y$, material constants D and μ , the resonance frequencies are [11]

$$\omega_{mn} = \sqrt{\frac{D}{\mu}} [(m\pi/L_x)^2 + (n\pi/L_y)^2], \quad m, n = 1, 2, 3, \dots, \tag{32}$$

where m and n are integers. The eigenfunctions of the panel are

$$\phi_{mn}(x, y) = \frac{2}{\sqrt{L_x L_y}} \sin(m\pi x/L_x) \sin(n\pi y/L_y), \quad m, n = 1, 2, 3, \dots \tag{33}$$

The panel is divided into 121 elements, as shown in Fig. 4. Assume that two exciters are mounted on the 58th and the 64th elements in Fig. 4. The voice-coil resistance is 4Ω and the input voltage

Table 1
Parameters of the panel and the exciter

	Parameters
Panel	Young's modulus $E = 2.28 \times 10^9 \text{ N/m}^2$ Bending stiffness $D = 26.625 \text{ N m}$ Area density $\mu = 0.741 \text{ kg/m}^2$ Dimension = $0.27 \text{ m} \times 0.27 \text{ m} \times 0.005 \text{ m}$ Poisson ratio $\nu = 0.33$
Exciter	Impedance of voice coil $Z_c = 4 + j\omega 32 \times 10^{-6} \Omega$ Motor constant $Bl = 2.35 \text{ Wb/m}$ Compliance of coil suspension $C_s = 297 \times 10^{-6} \text{ m/N}$ Damping of panel suspension $R_s = 0.257 \text{ N s/m}$ Mass of magnet $M_m = 37 \times 10^{-3} \text{ kg}$ Mass of coil $M_c = 0.72 \times 10^{-3} \text{ kg}$

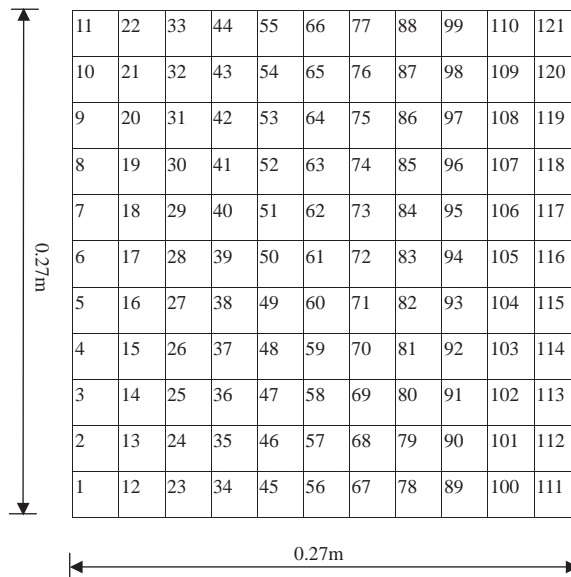


Fig. 4. Mesh structure of the panel discretized into 121 elements.

is $2V_{r.m.s.}$, which amounts to 1 W input power. The sound pressure level at a distance of 1 m on the central axis from the panel, calculated using the aforementioned numerical model, is plotted against frequency in Fig. 5. The approach neglecting the acoustic loading is also calculated for comparison. The effect due to acoustic loading is evidenced from the results: the peaks are decreased (damping) and the resonance frequencies are lowered (mass loading) when the acoustic coupling is incorporated into the model. For the same panel speaker, the sound power and the directional response are also calculated and shown in Figs. 6 and 7. These are not optimized results, but are only meant to show the capability of the developed numerical model.

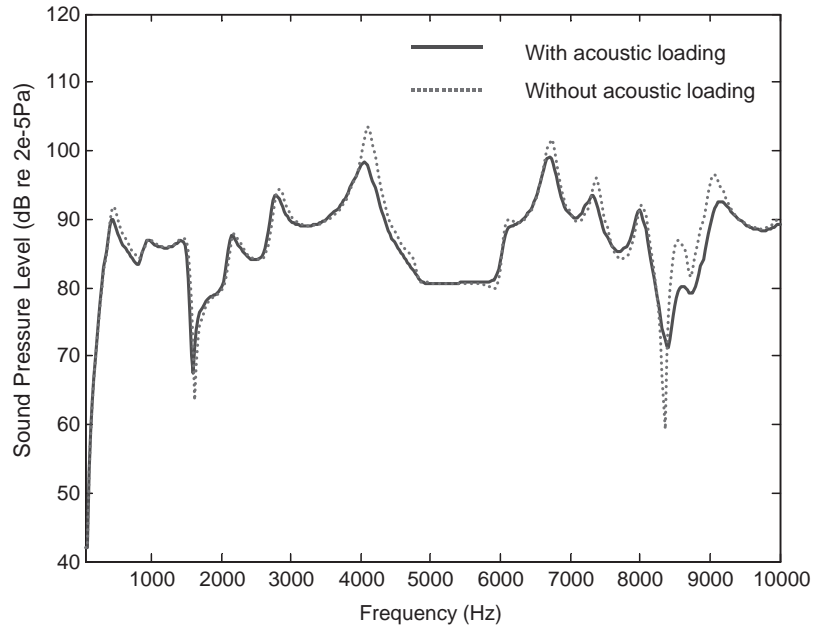


Fig. 5. Simulation of the sound pressure level of the panel speaker. The results pertaining to the condition with acoustic loading (solid line) and without acoustic loading (dotted line) are compared.

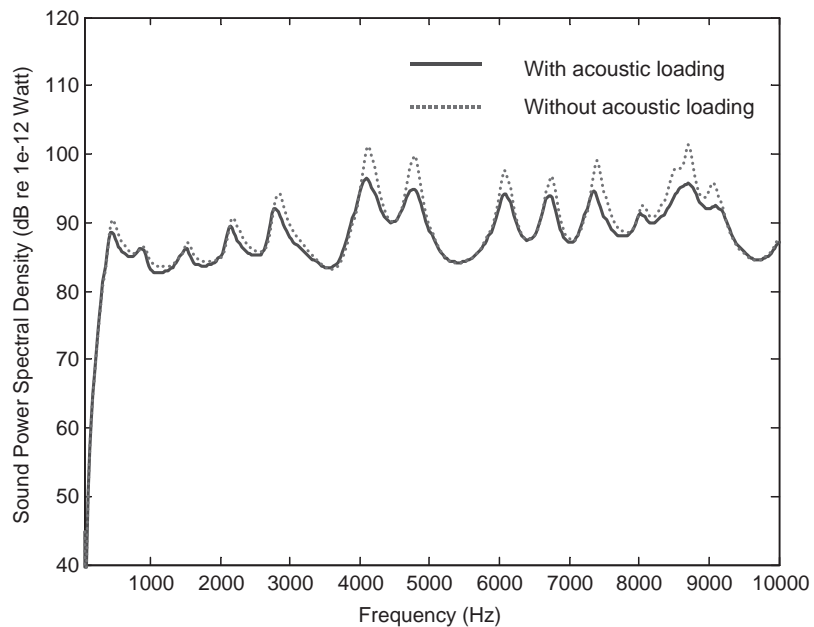


Fig. 6. Simulation of the sound power spectral density of the panel speaker. The results pertaining to the condition with acoustic loading (solid line) and without acoustic loading (dot line) are compared.

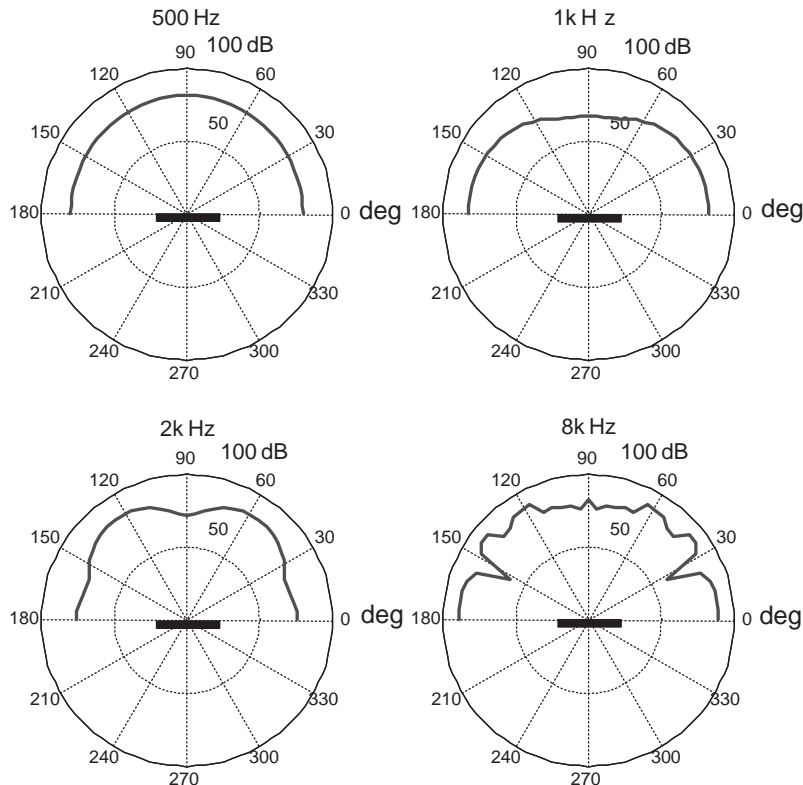


Fig. 7. Simulation of directional response of the panel speaker with two exciters located at the 58th and 64th elements.

3. Optimization using GA

In this section, a systematic procedure using GA intended for optimal design of the panel speakers is presented. The goal is to maximize omni-directionality and the efficiency by adjusting the positions to mount exciters and electronic delay to each exciter. GA is a search technique based on the evolution theory. A typical GA procedure consists of a string representation (genes) of the nodes in the search space, a fitness function to evaluate, three genetic operators for generating new search nodes, and a stochastic assignment to control the genetic operators. GA is particularly effective in non-convex optimization owing to its multiple-starting-points nature. In this paper, we wish to find a design with omni-directional responses, applicable in a wide frequency range. Thus, the center frequencies (from 31.5 Hz to 16 kHz) of octave band filters [12] are chosen for the calculation in optimization. The flow chart of the GA procedure in Fig. 8 consists of the following steps:

(1) *Initialization*: An initial population of search nodes is randomly generated. In this paper, the design variables are the positions of exciters and the delay of input signal to each exciter. From Fig. 4, there are 121 possible positions of exciters. We also restrict the sample delay of the input signal to be $0 \leq N \leq 90$. The sampling rate is assumed as 25 kHz. Assume that three exciters are

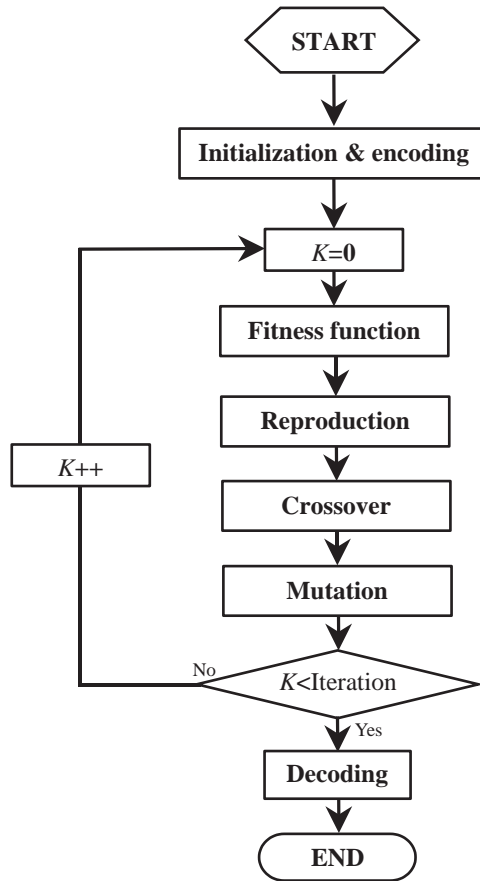


Fig. 8. Flowchart of the GA-based optimization procedure.

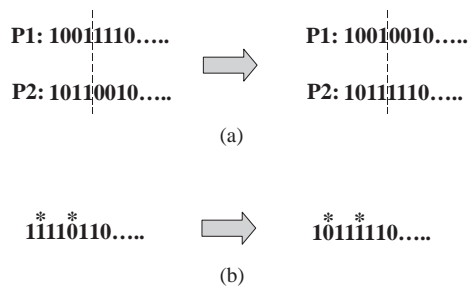


Fig. 9. Illustration of the GA operators in binary codes: (a) crossover and (b) mutation.

used in the simulation, among which two of them have the same delay and are located at symmetrical positions. The positions and the delays are then encoded into binary strings called *chromosomes*, as shown in Fig. 9(a). The population includes 100 genes and the iteration number of GA is set to be 200.

(2) *Fitness function*: Define the spatial flatness function

$$G = \frac{1}{K} \sum_{j=1}^K \sum_{i=1}^L [g_i(\omega_j)^2 - Lg_{mean}(\omega_j)^2], \quad (34)$$

where K is the number of frequencies, L is the number of the field points along a semi-circle, $g_i(\omega_j)$ is the sound pressure of the point i along the semi-circle at the frequency ω_j , and $g_{mean}(\omega_j)$ is the mean of the sound pressures at the frequency ω_j . A small value of spatial flatness function corresponds to good omni-directionality. Next, define the efficiency function

$$Y = \frac{1}{K} \sum_{j=1}^K W(\omega_j), \quad (35)$$

where $W(\omega_j)$ is the sound power at the frequency ω_j . A large value of efficiency function is most desirable, though this generally contradicts the requirement of the omni-directionality. Now, combining the spatial flatness and the efficiency yields the fitness function for the GA procedure:

$$Q = Y/G. \quad (36)$$

(3) *Reproduction*: Based on the fitness values of the strings in the population, a new pool of population of strings is produced for the subsequent genetic operations. Strings with larger fitness values are more likely to reproduce.

(4) *Crossover*: The crossover operator allows the reproduction of new strings through combination of parts of strings. A simple crossover operation is done by swapping parts of a pair

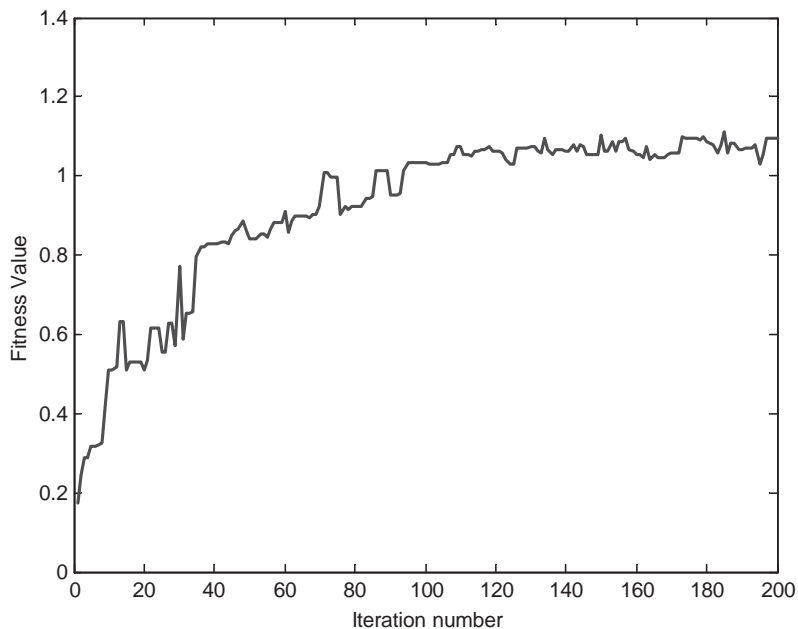


Fig. 10. Learning curve of the GA procedure. The fitness function converges after approximately 100 iterations.

of strings to form a new pair of strings. Pairs of strings are randomly selected for mating, and the splice point of a string where the swapping takes place is also randomly selected (Fig. 9(a)).

(5) *Mutation*: Mutation is the sporadic alteration of chromosomes. Mutation is performed by inverting a bit in the binary code (Fig. 9(b)). The position at which the bit is inverted is randomly selected with a small probability.

(6) Repeat Steps (2)–(5) until a convergence limit or a pre-specified number of iterations has been reached.

Fig. 10 shows the learning curve of the GA procedure applied to our problem. The fitness function starts to converge after approximately 100 iterations. As the genes are decoded into physical variables, the optimal positions are found to locate at the 63rd, 47th and 69th elements with sample delays $N = 0, 3$ and 3 , respectively.

4. Experimental investigations

To verify the proposed GA-based optimization technique, experimental investigations are carried out in the laboratory. To minimize the effect of room response, the experiment data are measured in an anechoic room. Fig. 11 shows the experimental arrangement. Recall that, in simulation, the panel is assumed to be simply supported, which is difficult to realize in practice. Instead, an adhesive tape is used in the experiment to fix the boundary of the panel.

In the experiment, ISO 3745 was employed for measuring the sound power in the anechoic room [13]. Directional response of the panel speaker was measured by using an automated turntable depicted in Fig. 12. A stepping motor controlled by a PC rotates the turntable on which the panel speaker was mounted. The motor rotates from 0° to 180° with 1° increments. The measuring microphone is positioned at a distance of 2 m away from the turntable. The voltage input to each exciter is $2 V_{r.m.s.}$. A digital signal processor (DSP, TMS320C31) was utilized to

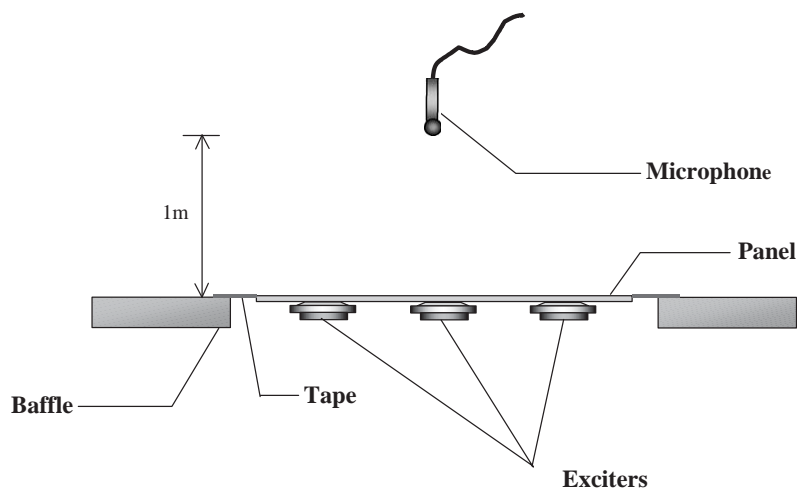


Fig. 11. Experimental arrangement of the panel speaker. An adhesive tape is used to suspend the panel within a rigid baffle.

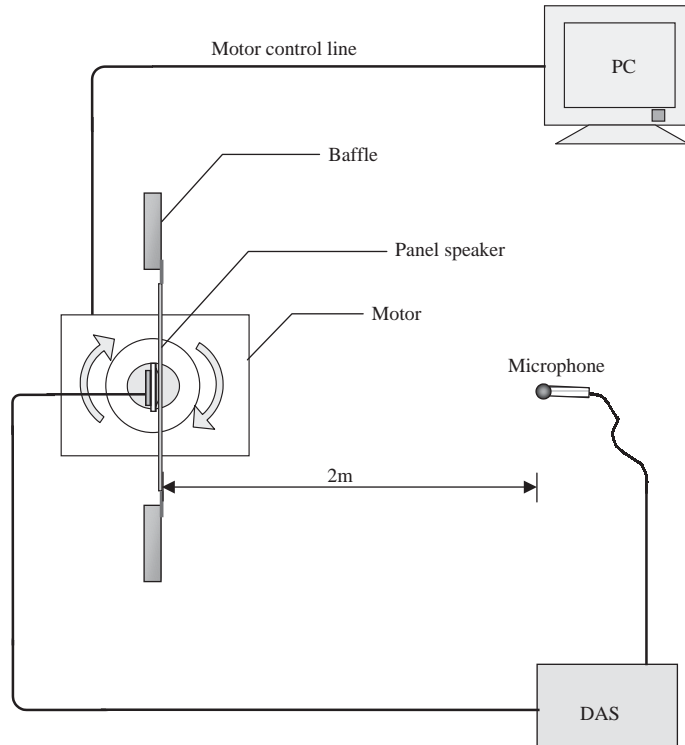


Fig. 12. Experimental arrangement for measuring the directional response of the panel speaker. A turntable is rotated by a stepping motor. A data acquisition system is used to measure the signal from the microphone. The overall signal processing activity is monitored by a personal computer.

produce the electronic delay ($N = 3$), as required in the optimal design, of the input signal to the exciters. The optimal positions of the 63rd, 47th and 69th elements found in the GA procedure were selected in the experiment to mount the exciters. For comparison, a configuration where the exciters are mounted on an arbitrarily chosen “non-optimal” positions, the 61th, 38th and 82nd elements, without delay was also tested. Fig. 13 compares the directional response of the optimal design to that of the non-optimal design. From the results, it is observed that the optimal design produced an improved omni-directionality as compared to the non-optimal design. In particular, this is reflected in the flatness of the beam pattern in 500 and 1 kHz. In 2 and 4 kHz, the optimal design appears to generate a pattern with an angle wider than the non-optimal design. Table 2 compares the sound power measured by ISO3745 between the optimal design and the non-optimal design. The optimal design was found to radiate unanimously higher acoustic output than the non-optimal design at all frequencies. Not only this case but also several other choices of exciter setting, as not presented here, produced inferior performance than the optimal configuration. Therefore, it is concluded that the GA-based optimization procedure indeed has produced a design of panel speaker with improved performance in terms of omni-directionality and efficiency.

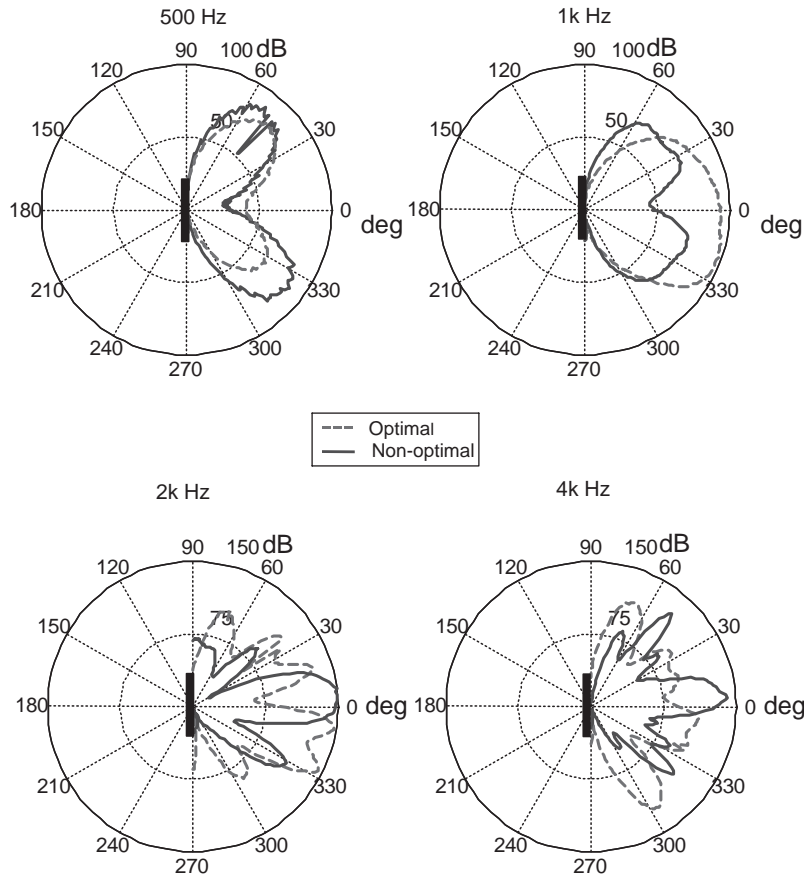


Fig. 13. Comparison of directional responses between the optimal design (dashed line) and a non-optimal design (solid line) of the panel speaker. The directional responses are measured at the frequencies 500 Hz, 1, 2 and 4 kHz.

Table 2

Comparison of the experimental results of the sound power between the optimal design and the non-optimal design (dB re. 1×10^{-12} W)

	500 Hz	1 kHz	2 kHz	4 kHz
Optimal	92.5	94.7	95.3	91.6
Non-optimal	91.8	93.7	93.9	88.3

5. Conclusions

The principal outcome of this work can be summarized in two aspects. First, a fully coupled model of the panel speaker has been established for simulation. Second, a GA-based procedure has been developed for obtaining the optimal design. The present simulation model takes into account the acoustic loading on the light panel structures. The impedance matrices of the exciter, the panel and the medium are combined into one matrix in the formulation. The assumed-modes

method was used in the model, which provides an efficient means for response computation. On the basis of the simulation model, a search scheme was exploited to optimize, by using the GA, the efficiency and omni-directionality of panel speaker. The GA procedure produces the optimal positions to mount exciters and the electronic delay to the input signals. The thus obtained optimal configuration of the panel speaker has been verified by experiments. The experimental result indicates that the performance was enhanced by means of the optimization design approach.

As a limitation of the present work, eigenfunctions of simply supported plates are used in the assumed-modes expansion. It is usually difficult to derive a dynamic model for more general problems by using assumed-modes method which is only practical for simple boundary conditions. A finite-element-based model that is able to handle complex boundary conditions is currently being developed to improve the design optimization.

Acknowledgements

Thanks are due to the illuminating discussions with NXT, New Transducers Ltd., UK. The work was supported by the *National Science Council (NSC)* in Taiwan, under the Project Number NSC 89-2212-E009-057.

References

- [1] H. Azima, NXT up against wall, *Audio Magazine* (1998) 34–41.
- [2] M.R. Bai, T. Huang, Development of panel loudspeaker system: design, Evaluation and enhancement, *Journal of the Acoustical Society of America* 109 (2001) 2751–2761.
- [3] M.C. Junger, D. Feit, *Sound, Structure, and Their Interaction*, The MIT Press, Cambridge, MA, 1986.
- [4] F. Fahy, *Sound and Structural Vibration*, Academic Press, London, 1985.
- [5] L. Cremer, M. Heckl, *Structure-born Sound*, Springer, Berlin, 1988.
- [6] R. Caponetto, L. Fortuna, G. Muscato, G. Nunnari, Search of optimal realization matrix for filter implementation by using a genetic algorithm, *IEEE Transactions on Systems, Man and Cybernetics* 20 (2) (1993) 471–474.
- [7] B.H. Tongue, *Principles of Vibration*, Oxford University Press, Oxford, UK, 1996.
- [8] Y. Kagawa, T. Tsuchiya, N. Wakatsuki, Equivalent circuit representation of a vibrating structure with piezoelectric transducers and the stability consideration in the active damping control, *Int. J. of Smart Material and Structures* 10 (2001) 389–394.
- [9] F.S. Tse, I.E. Morse, R.T. Hinkle, *Mechanical Vibrations Theory and Applications*, Allyn & Bacon, Newton, MA, 1978.
- [10] A.P. Berkhoff, Sensor Scheme Design for Active Structural Acoustic Control, *Journal of the Acoustical Society of America* 108 (2000) 1037–1045.
- [11] A.W. Leissa, *Vibration of Plates*, Acoustical Society of America, Woodbury, NY, 1993.
- [12] A.D. Pierce, *Acoustics*, McGraw-Hill, New York, 1981.
- [13] ISO standard, Basic array of microphone positions in free field over a reflecting plane, ISO-3745-1977 (E), 1977.